Communication

TiO2-Coated Meltblown Nonwoven Fabrics Prepared via Atomic Layer Deposition for the Inactivation of *E. coli* as a Model Photocatalytic Drinking Water Treatment System

Alexander G. Aragon [1,2], Jaime A. Cárdenas Sánchez [2,3], Carlos Zimeri [4], Eunkyoung Shim [4], Xiaomeng Fang [4] and Kyana R. L. Young [2,*]

[1] Department of Chemistry, Wake Forest University, 1834 Wake Forest Road, Winston-Salem, NC 27109, USA; aaragon@forsythtech.edu
[2] Department of Engineering, Wake Forest University, 455 Vine Street, Winston-Salem, NC 27101, USA; cardja20@wfu.edu
[3] Department of Biology, Wake Forest University, 1834 Wake Forest Road, Winston-Salem, NC 27109, USA
[4] Department of Textile Engineering, Chemistry and Science, North Carolina State University, 1020 Main Campus Drive, Raleigh, NC 27606, USA; cjzimeri@ncsu.edu (C.Z.); eshim@ncsu.edu (E.S.); xfang3@ncsu.edu (X.F.)
[*] Correspondence: youngk@wfu.edu

Abstract: The controlled manufacturing of semiconductor photocatalysts is crucial to their development for drinking water treatment. In this study, TiO2-coated meltblown nonwoven fabrics prepared via Atomic Layer Deposition (ALD) are applied for the inactivation of *Escherichia coli* (*E. coli*). It is observed that in the presence of an ultraviolet light-emitting diode (UV-LED) light source (255 nm), 1.35 log *E. coli* inactivation is achieved. However, exposure to catalyst-coated fabrics in addition to the light source resulted in >4 log *E. coli* inactivation, suggesting a much higher rate of hydroxyl radical formation on the surface, leading to cell death.

Keywords: antimicrobial; nonwovens; drinking water; atomic layer deposition; photocatalysis

1. Introduction

Water is an essential natural resource and is humanity's greatest need for the sustenance of life for continued health, wellbeing and development [1,2]. Unfortunately, 20% of the world's population has no access to clean drinking water, and this remains an issue due to the increased global population in recent years [3,4]. Many types of water contaminants exist, such as chemical waste, heavy metals, and biological agents such as disease-causing microbes. In most cases where clean water is inaccessible, the greatest concern is disease, such as cholera, typhus, polio, tuberculosis, diphtheria and diarrhea [5]. One such microbe that signals issues with water quality is *Escherichia coli* (*E. coli*). *E. coli* serves as an indicator microbe to verify the presence of fecal indicator organisms, and thus serves as a good model for testing disinfection methods. It is crucial to develop drinking water treatment methods that inactivate these organisms in both a safe and sustainable way, and utilizing *E. coli* as a model allows for ease of testing.

Drinking water disinfection methods, including chlorination, ozonation, radiation, advanced filtration and the use of ultraviolet (UV) light, are common technologies employed in drinking water treatment [2,6]. However, there are several key drawbacks in using these conventional methods, such as the formation of disinfection byproducts that are potentially toxic/carcinogenic, high operational and maintenance costs, the development of antibiotic drug resistance over time, and a low disinfection efficiency [2,3,5,7,8]. These methods are also met with implementation challenges, and thus alternative methods must be sought to achieve truly sustainable, low-cost, and minimally toxic water treatment methods. Photocatalytic disinfection remains an innovative and promising option for water

purification that removes some of these challenges [3,9]. Given the minimal operational cost and highly sustainable nature of photocatalysis, the development of catalysts utilized for this type of disinfection is a current area of research with high interest [4].

Traditional photocatalysis utilizes semiconductor materials, such as metal oxides [10–12], perovskite oxides [13,14], and metal chalcogenides [10,15], that are synthesized chemically with the use of potentially toxic reagents. These catalysts are typically also produced in bulk powders or thin films, where surface area and reproducibility concerns arise in terms of large-scale water treatment usage. Therefore, it is crucial to develop methods to produce semiconductor photocatalysts with a high uniformity, minimal toxicity, and high surface area for industrial use. ALD provides strong levels of controllability and uniformity to produce such semiconductor photocatalysts, including TiO_2, which is utilized in this study. To date, metal oxides have been heavily studied as antibacterial agents prepared via traditional chemical methods [16,17], and the preparation of TiO_2 and ZnO via ALD shows promise for the large-scale production of photocatalysts for drinking water treatment.

ALD is a powerful tool for the atomically precise design and synthesis of catalytic materials. It is key to developing new technologies to produce valuable products from resources including fossil fuel, biomass, carbon dioxide and water. Large industries, such as energy, pharmaceuticals, food processing, and environmental remediation, all use ALD because of the improved uniformity and control it provides for creating advanced systems. TiO_2 is a very common material for these applications in electronics and pharmaceuticals, such as bacterial inactivation [18]. ALD has been shown to be effective at controlling metal and metal oxide active sites and improving catalytic activity, selectivity, and longevity. To date, there have been a few key applications of ALD in catalysis, including the photocatalytic degradation of organic pollutants and production of carbon dioxide, to name a few [19,20]. In this work, the utilization of TiO_2 deposited via ALD saw much greater efficiency gains and stronger stability due to the increased attachment on the surface of the substrates used. This highlights the strong potential of ALD as a method to produce effective and stable catalysts, but more work is needed to improve the cost-effectiveness of the production and understand the mechanisms by which they operate.

In this study, nano-TiO_2 was attached to the surface of meltblown nonwoven fabrics via ALD methods to prepare a photocatalyst for the inactivation of *E. coli* in water. Textiles have been shown to also be useful for antimicrobial treatment [21,22] and thus can be seen as a strong substrate choice for the preparation of photocatalytic disinfection technologies based on ALD. Due to the near-zero waste of raw materials and environmental pollution, ALD proves to be a high-value synthetic process for the development of antibacterial textiles [22,23]. The overall structural properties of thin films on meltblown nonwoven fabrics are discussed to understand the deposition process and confirm the uniform synthesis of TiO_2 on the surface. The photocatalytic activity of catalyst-coated meltblown nonwoven fabrics is discussed and compared to a UV-LED light source alone. Lastly, the overall stability of catalyst films is discussed with respect to reusability.

2. Materials and Methods

2.1. Bacterial Stock Preparation

E. coli was used as the model bacterial microbial contaminant to assess the inactivation efficacy of the ALD photocatalyst on the meltblown nonwoven fabric. *E. coli* BA-1883 (American Type Culture Collection, Manassas, VA, USA) was aseptically transferred to Nutrient Broth (Difco™, Franklin Lakes, NJ, USA) and placed in an incubator at 37 °C for 5 h. The bacterial growth was then centrifuged at 2000 rpm for 2 min, with the supernatant being disposed and fresh phosphate buffered saline (PBS) added to resuspend the pellet. The pellet and PBS mixture were vortexed and centrifuged at 2000 rpm for 2 min; the supernatant was disposed, and fresh PBS was added, bringing the *E. coli* stock concentration to 10^6 colony-forming units (cfu) per milliliter.

2.2. Preparation of Meltblown Nonwoven Fabrics

The meltblown nonwoven fabrics used in this study were produced using a pilot-scale Reicofil$^{®®}$ (Reifenhauser, Troisdorf, Germany) meltblown line equipped with a traditional Exxon-style die (die orifice diameter = 400 μm, die orifice density = 35 holes/inch, setback = 1.2 mm, total die width = 1.3 m). Processing parameters were varied to control the meltblown fabric structures and are summarized in Table S1, with detailed structural characteristics shown in Table S2 (Supplementary Materials).

2.3. Synthesis of TiO$_2$ Films

The synthesis of TiO$_2$ films was done via ALD methods utilizing an Arradiance GEMSTAR-6 benchtop chamber equipped with a furnace. Fabric samples along with a Si reference wafer were placed into the chamber, and the sequential depositions of Ti (titanium isopropoxide) and O (deionized water, Milli-Q, Randolph, MA, USA) were done chemically. The deposition conditions included a chamber temperature of 150 °C with a Ti pulse time of 100 ms followed by a N$_2$ purge of 23 s and with an O pulse time of 1000 ms followed by another N$_2$ purge of 28 s to complete a cycle (growth rate = 0.03 nm/cycle). The full growth of the films was measured via XRR experiments utilizing a Bruker D8 Discover X-ray diffractometer equipped with Cu kα radiation and a Goebel mirror.

2.4. Photocatalytic Studies

2.4.1. Ultraviolet Light-Emitting Diode Irradiation

For disinfection, a UV-LED (PearlBeam™, AquiSense Technologies, Erlanger, KY, USA) was used as a light source. Detection of irradiance was conducted utilizing the ILT-5000 radiometer, equipped with an SED 270/QT detector (International Light Technologies, Peabody, MA, USA). For irradiance of the water sample, a reflection factor = 0.975, petri factor = 0.894, water factor = 0.981, and divergence factor = 0.975 were used to correct the irradiance values. The irradiance at the water surface is 0.041 mW/cm^2.

2.4.2. Experimental Conditions

An aliquot of 1.5 mL of the *E. coli* stock was added to 13.5 mL of Milli-Q water (25 °C, 18.2 Ω) in a glass 60 × 15 mm quartz Petri dish and placed on a magnetic stir plate to gently mix at 250 rpm. The Petri dish was placed under a collimated beam for 60 s, where the UV-LED irradiated the sample at $λ$ = 255 nm, selected for its proximity to the peak absorbance ($λ$ = 254 nm) responsible for DNA damage. Simultaneously, the meltblown nonwoven fabric was added to the Petri dish, and the UV-LED was powered on. At the conclusion of irradiation, the meltblown nonwoven fabric was then removed from the Petri dish, and the solution was processed using the membrane filtration method (Standard Methods 9222B); the filter was placed on m-Endo Agar LES (Remel™, Lenexa, KS, USA) in the incubator for 24 h at 37 °C and then transferred to the EC Medium w/MUG (Remel™, Lenexa, KS, USA) for 4 h at 44 °C. After incubation, fluorescent colonies were quantified using the plate count method. The control groups were Milli-Q (negative) and bacteria stock solution (positive). The experimental groups were meltblown nonwoven fabric, meltblown nonwoven fabric deposited with photocatalyst, meltblown nonwoven fabric deposited with photocatalyst and UV-LED-irradiated, Laprotex™, Laprotex™ deposited with photocatalyst, Laprotex™ deposited with photocatalyst and UV-LED-irradiated, photocatalyst, photocatalyst irradiated with UV-LED, and UV-LED.
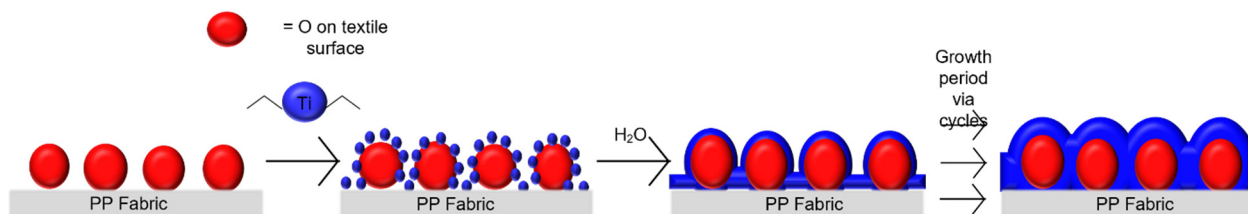
2.4.3. Inactivation Kinetics

The *log inactivation* for the *E. coli* was determined via Equation (1), where N_0 is the initial concentration of cfu/mL with no irradiation and N_f is the concentration of cfu/mL after UV-LED irradiation:

$$log \frac{N_f}{N_0} = log\ inactivation \tag{1}$$

A comparison of log inactivation was conducted to assess the inactivation efficacy of the experimental conditions. Data for TiO_2 were collected in triplicate.

3. Results and Discussion

Thin films of TiO_2 were deposited on the polypropylene-based nonwovens via ALD, and a full cycle of ALD is pictured in Scheme 1.

Scheme 1. ALD deposition cycle on nonwoven fabric surface.

The Ti precursor first reacts with hydroxyl groups on the surface of the meltblown nonwoven fabrics, followed by a reaction between this intermediate product and the water precursor to form a layer of TiO_2 on the surface. The thickness of these films can be adjusted via the number of ALD cycles run, but for this work, an average film thickness of ~12 nm was utilized for the TiO_2 films, as determined via XRR experiments shown in Figure S1 (Supplementary Materials). In addition to the determination of the film thickness, which gives an idea of the load of TiO_2, a more exact quantification of the TiO_2 concentration via TGA analysis should be done in the future to fully understand the impact of the TiO_2 load on the disinfection efficiency of the coated fabrics.

The morphology of ALD-treated nonwovens compared to a pristine nonwoven fiber is shown in Figure 1a,b and was obtained via SEM imaging.
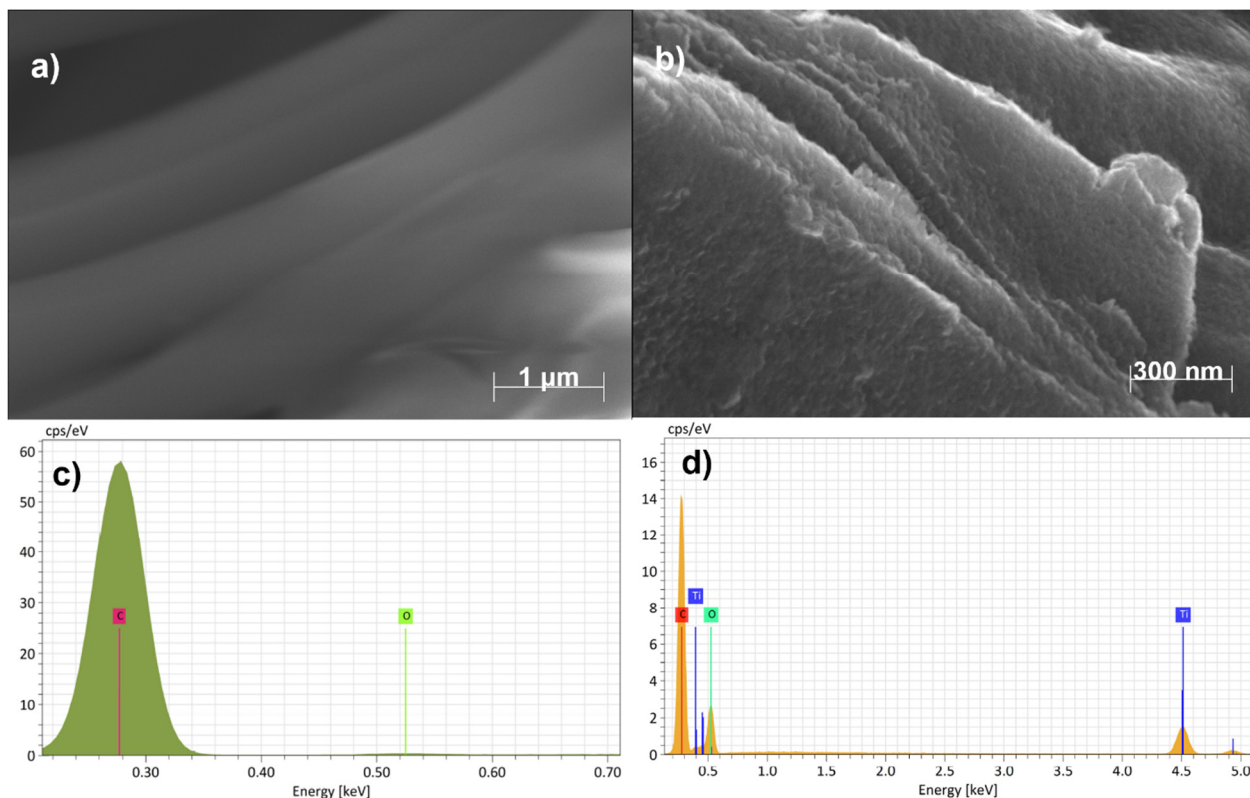

Figure 1. (**a**) SEM image of pristine fabric; (**b**) SEM image of TiO_2-coated fabric; (**c**) EDS spectrum of pristine fabric; (**d**) EDS spectrum of TiO_2-coated fabric.

A rough surface of metal oxide coating is achieved after the ALD process when comparing the pristine fiber to TiO_2-coated nonwovens, respectively. The SEM images were collected in triplicate over a series of three meltblown nonwoven fabric samples, and the TiO_2 films were found to be amorphous, which is consistent with other literature reports of low-temperature ALD TiO_2 films [24,25]. The EDS spectra shown in Figure 1c,d, collected over the series of meltblown fabrics, paired with line scan data shown in Figure S2 (Supplementary Materials) suggest that Ti is present on the surface of the meltblown nonwoven fabrics after ALD and is present in the same regions as O on the surface. The morphology and elemental composition of ALD films deposited on the commercially available tested textile are shown in Figure S3 (Supplementary Materials).

To confirm the successful deposition of TiO_2 on the surface of the meltblown nonwoven fabrics, both X-ray photoelectron spectroscopy (XPS) and IR spectroscopy were utilized to probe the chemical structure of the pristine and ALD-treated meltblown nonwoven fabrics.

The IR spectrum of the treated and pristine nonwovens is shown in Figure 2a. The peaks at 2900, 1350, and 1053 cm^{-1} represent the stretch vibrations of C-H, O-H, and C=C bonds, respectively. After ALD treatment, a broad peak is present near 3500 cm^{-1}, which represents the Ti-OH stretch vibration, while the broad feature observed below 1000 cm^{-1} is the Ti-O-Ti stretch and suggests deposition of TiO_2 on the surface of the meltblown nonwoven fabric. The C 1s and O 1s characteristic peaks appear at 284 and 532 eV, respectively, for the pristine nonwoven fabric, as shown in the XPS survey spectrum in Figure 2b. When compared to the TiO_2-coated meltblown nonwoven fabrics, the presence of the characteristic Ti 2p peak at 458 eV further suggests the successful deposition of TiO_2 on the surface.
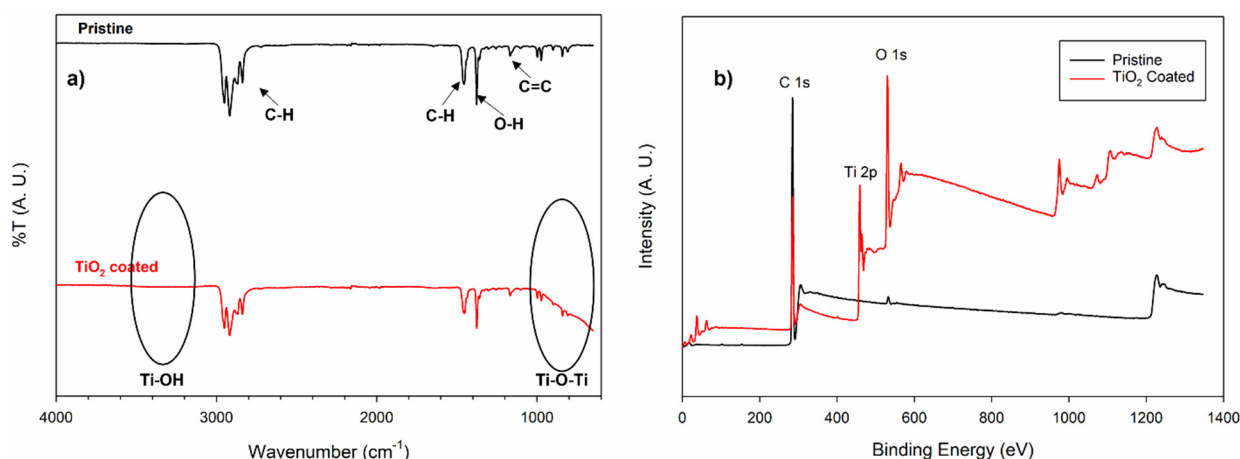

Figure 2. (**a**) IR spectrum of pristine and ALDtreated meltblown nonwoven fabrics; (**b**) XPS survey spectrum of pristine and ALD-treated meltblown nonwoven fabrics.

In photocatalytic systems, the application of external light provides the energy to move electrons from the valence band to the conduction band; this movement of electrons allows the production of powerful oxidants (hydroxyl radicals) in a bulk water system. The oxidant causes damage to the DNA of waterborne microbes, thus rendering them inactive and unable to reproduce. The use of UV-LED as an external light source was analyzed as a singular treatment mechanism and compared to light-irradiated photocatalysts for the disinfection of bulk water samples. The samples tested were at pH 7 and temperature = 25 °C, and a collimated beam of UV-LED at λ = 255 nm (intensity = 0.041 mW/cm^2) was utilized to assess the efficacy of the *E. coli* inactivation of TiO_2-coated fabrics. An overview of the photoreactor setup is shown in Figure 3a.
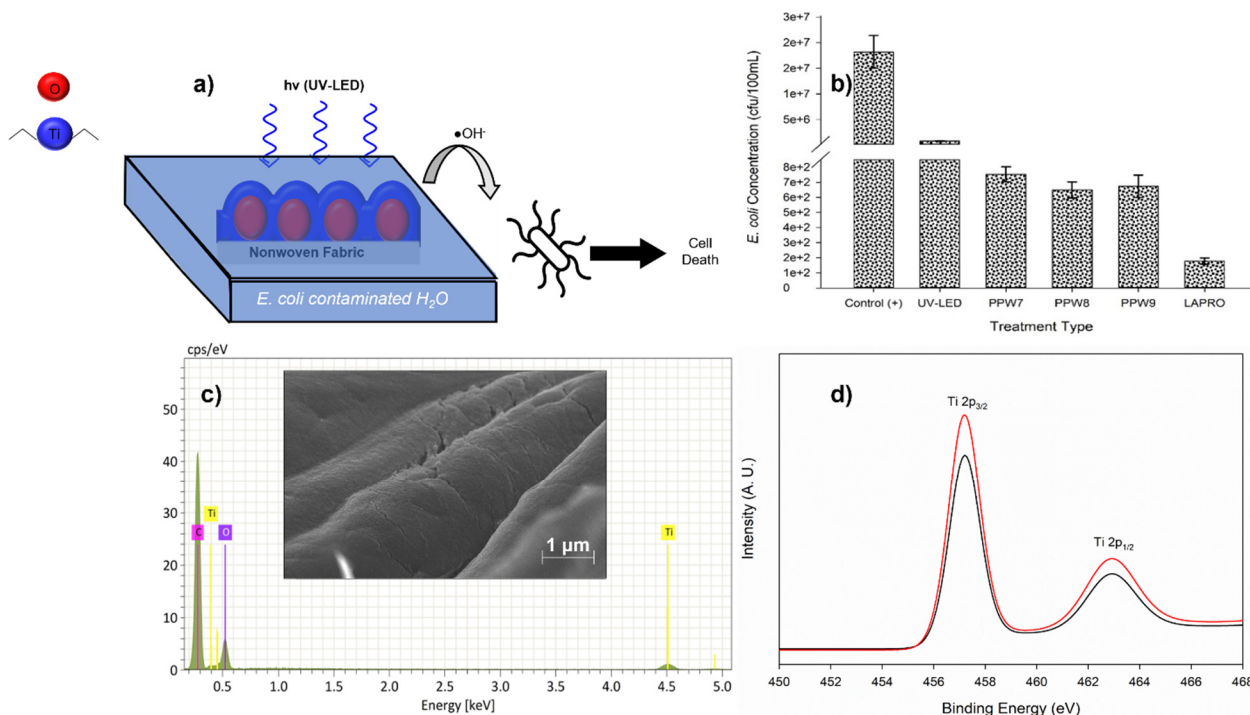
Figure 3. (**a**) Overview of photoreactor setup used for photocatalytic experiments (Conditions: pH = 7, temperature = 25 °C, λ = 255 nm, dose = 2.46 mJ/cm^2); (**b**) E. coli concentration after exposure to UV-LED alone or TiO$_2$-coated meltblown nonwoven with UV-LED irradiation (*n* = 3); (**c**) EDS spectrum and SEM image (inset) of TiO$_2$-coated meltblown nonwoven fabric after catalysis; (**d**) XPS spectrum for the Ti 2p electron before (black) and after (red) catalysis for TiO$_2$-coated nonwoven fabric.

When exclusively irradiating the bulk water with UV-LED, UV dose = 2.46 mJ/cm^2 (0.041 mW/cm^2 × 60 s), 1.35 ± 0.0422 log inactivation of *E. coli* was achieved (Table 1).

Table 1. Comparison of log inactivation for experimental types of *E. coli* inactivation.

Fabric Type	Catalyst	External Light	Log Inactivation
PPW7	TiO$_2$	UV-LED	4.40 ± 0.043
PPW8	TiO$_2$	UV-LED	4.40 ± 0.032
PPW9	TiO$_2$	UV-LED	4.40 ± 0.041
Laprotex™	TiO$_2$	UV-LED	5.00 ± 0.031
-	-	UV-LED	1.35 ± 0.0422

For experiments performed when the photocatalyst was deposited on the meltblown nonwoven fabric, inactivation of *E. coli* was evident (Figure 3b). The PPW7, PPW8, and PPW9 deposited with TiO$_2$ and a UV dose = 2.46 mJ/cm^2 achieved a minimum of 4.40 ± 0.032 log inactivation of *E. coli*. The significant improvement in log *E. coli* inactivation for the coated meltblown nonwovens suggests a high potential for the utilization of this technology as a multifunctional drinking water treatment option. For the comparison of the treatment efficacy between fabric types and TiO$_2$, the bacteria inactivation was impacted by the commercial Laprotex™ fabric (*p* < 0.001) compared to the insignificant difference when using the PPW fabrics (*p* = 0.260). These findings suggest the strong potential shown by the coated meltblown nonwoven fabrics for drinking water treatment, and further work is needed to test their capability under different irradiation sources, such as UVA-LED, which is more cost-effective than UVC-LED. Another factor that can significantly impact the photocatalytic efficiency is the exact load of TiO$_2$ on the meltblown nonwoven fabric, and future studies would also utilize TGA analyses to determine this. Though the mechanism of photocatalytic inactivation is not yet fully understood, it is believed that through the

creation of hydroxyl and superoxide radicals on the surface of the catalyst in solution, direct oxidative damage of the DNA of *E. coli* is achieved, following previous literature reports [26]. Density Functional Theory calculations are needed to understand the band structure, differential charge density, and density of states for the catalyst-coated nonwoven fabrics to probe the movement of photogenerated radical oxidants on the surface.

The stability of the as-synthesized TiO_2 thin film catalysts was probed to determine the reusability of the coated meltblown nonwoven fabrics for larger scale use. Figure 3c details the morphology and elemental composition of the TiO_2-coated nonwovens after catalysis. The overall film morphology remains relativity unchanged after catalysis. As evidenced by the EDS spectrum, the TiO_2 films remain relatively unchanged given the presence of the Ti in the spectra. To further examine the change in catalyst films during catalysis, XPS was utilized to probe the changes in the chemical structure of TiO_2 and is shown in Figure 3d. The spectrum for the Ti 2p electron shows no change in the characteristic peaks of Ti (IV) for the TiO_2-treated nonwoven fabric, which suggests a strong stability and reusability of the TiO_2 catalyst. Detailed atomic percentages as determined via XPS are shown in the Supplementary Materials (Table S3). Although there is not much change in the films, as evidenced through the post-catalysis EDS and XPS spectra, work is still needed to fully examine the reusability of the coated fabrics through multiple cycles and in large scale drinking water treatment systems.

4. Conclusions

Uniform TiO_2 films were deposited on meltblown nonwovens via ALD and applied as a photocatalyst for the inactivation of *E. coli* in bulk water. It was found that the photocatalyst-coated meltblown nonwovens outperformed the UV-LED light source utilized, as evidenced by a near 4-fold increase in *E. coli* log inactivation for all fabrics tested with TiO_2. In addition, a significant difference of *E. coli* log inactivation between the Laprotex™ and PPW fabrics coated with TiO_2 was observed. This suggests that the bacterial inactivation was affected by the presence of the Laprotex™ fabric. Photocatalyst-coated films were shown to have great stability given the minimal change in the structural morphology and elemental composition of the coated fabrics after catalysis. The minimal change in the Ti 2p XPS spectrum suggests that TiO_2 films are completely intact after catalysis. The utilization of ALD for the preparation of catalysts shows a strong potential for the development of sustainable, low-environmental-impact drinking water treatment technologies in the next few years, and more work is needed to understand the reusability and efficacy under different irradiation sources of this technology and to improve its cost-effectiveness. Furthermore, the determination of the distinct hydroxyl radical groups produced in the photocatalytic process will allow for the continued exploration of photocatalysts suitable for this application.

Author Contributions: Conceptualization, A.G.A. and K.R.L.Y.; methodology, A.G.A., J.A.C.S. and C.Z.; validation, A.G.A. and K.R.L.Y.; formal analysis, A.G.A., C.Z. and K.R.L.Y.; investigation, A.G.A., J.A.C.S. and C.Z.; resources, E.S., X.F. and K.R.L.Y.; writing—original draft preparation, A.G.A.; writing—review and editing, E.S., X.F. and K.R.L.Y.; visualization, A.G.A. and K.R.L.Y.; supervision, E.S., X.F. and K.R.L.Y.; project administration, K.R.L.Y.; funding acquisition, K.R.L.Y. All authors have read and agreed to the published version of the manuscript.

References

1. Odonkor, S.T.; Ampofo, J.K. *Escherichia coli* as an Indicator of Bacteriological Quality of Water: An Overview. *Microbiol. Res.* **2013**, *4*, e2. [CrossRef]
2. Vietro, N.D.; Tursi, A.; Beneduci, A.; Chidichimo, F.; Milella, A.; Fracassi, F.; Chatzisymeon, E.; Chidichimo, G. Photocatalytic Inactivation of *Escherichia coli* Bacteria in Water Using Low Pressure Plasma Deposited TiO$_2$ Cellulose Fabric. *Photochem. Photobiol. Sci.* **2019**, *18*, 2248–2258. [CrossRef] [PubMed]
3. Park, J.; Kettleson, E.; An, W.-J.; Tang, Y.J.; Biswas, P. Inactivation of *E. coli* in Water Using Photocatalytic, Nanostructured Films Synthesized by Aerosol Routes. *Catalysts* **2013**, *3*, 247–260. [CrossRef]
4. Ajiboye, T.O.; Babalola, S.O.; Onwudiwe, D.C. Photocatalytic Inactivation as a Method of Elimination of *E. coli* from Drinking Water. *Appl. Sci.* **2021**, *11*, 1313. [CrossRef]
5. Khani, M.; Amin, N.A.S.; Hosseini, S.N.; Heidarrezaei, M. Kinetics Study of the Photocatalytic Inactivation of *Escherichia coli*. *IJNBM* **2016**, *6*, 139. [CrossRef]
6. Ribeiro, M.A.; Cruz, J.M.; Montagnolli, R.N.; Bidoia, E.D.; Lopes, P.R.M. Photocatalytic and Photoelectrochemical Inactivation of *Escherichia coli* and *Staphylococcus aureus*. *Water Supply* **2014**, *15*, 107–113. [CrossRef]
7. Dunlop, P.S.M.; Ciavola, M.; Rizzo, L.; McDowell, D.A.; Byrne, J.A. Effect of Photocatalysis on the Transfer of Antibiotic Resistance Genes in Urban Wastewater. *Catal. Today* **2015**, *240*, 55–60. [CrossRef]
8. Friedman, N.D.; Temkin, E.; Carmeli, Y. The Negative Impact of Antibiotic Resistance. *Clin. Microbiol. Infect.* **2016**, *22*, 416–422. [CrossRef]
9. Benabbou, A.K.; Derriche, Z.; Felix, C.; Lejeune, P.; Guillard, C. Photocatalytic Inactivation of *Escherischia Coli*: Effect of Concentration of TiO$_2$ and Microorganism, Nature, and Intensity of UV Irradiation. *Appl. Catal. B Environ.* **2007**, *76*, 257–263. [CrossRef]
10. Aragon, A.G.; Kierulf-Vieira, W.; Łęcki, T.; Zarębska, K.; Widera-Kalinowska, J.; Skompska, M. Synthesis and Application of N-Doped TiO$_2$/CdS/Poly(1,8-Diaminocarbazole) Composite for Photocatalytic Degradation of 4-Chlorophenol under Visible Light. *Electrochim. Acta* **2019**, *314*, 73–80. [CrossRef]
11. Badhe, R.A.; Ansari, A.; Garje, S.S. Study of Optical Properties of TiO$_2$ Nanoparticles and CdS@TiO$_2$ Nanocomposites and Their Use for Photocatalytic Degradation of Rhodamine B under Natural Light Irradiation. *Bull. Mater. Sci.* **2021**, *44*, 11. [CrossRef]
12. Madkour, M.; Allam, O.G.; Abdel Nazeer, A.; Amin, M.O.; Al-Hetlani, E. CeO$_2$-Based Nanoheterostructures with p–n and n–n Heterojunction Arrangements for Enhancing the Solar-Driven Photodegradation of Rhodamine 6G Dye. *J. Mater. Sci. Mater. Electron.* **2019**, *30*, 10857–10866. [CrossRef]
13. He, Z.; Sun, C.; Yang, S.; Ding, Y.; He, H.; Wang, Z. Photocatalytic Degradation of Rhodamine B by Bi$_2$WO$_6$ with Electron Accepting Agent under Microwave Irradiation: Mechanism and Pathway. *J. Hazard. Mater.* **2009**, *162*, 1477–1486. [CrossRef]
14. Olagunju, M.O.; Zahran, E.M.; Reed, J.M.; Zeynaloo, E.; Shukla, D.; Cohn, J.L.; Surnar, B.; Dhar, S.; Bachas, L.G.; Knecht, M.R. Halide Effects in BiVO$_4$/BiO$_X$ Heterostructures Decorated with Pd Nanoparticles for Photocatalytic Degradation of Rhodamine B as a Model Organic Pollutant. *ACS Appl. Nano Mater.* **2021**, *4*, 3262–3272. [CrossRef]
15. Bessekhouad, Y.; Chaoui, N.; Trzpit, M.; Ghazzal, N.; Robert, D.; Weber, J.V. UV–Vis versus Visible Degradation of Acid Orange II in a Coupled CdS/TiO$_2$ Semiconductors Suspension. *J. Photochem. Photobiol. A Chem.* **2006**, *183*, 218–224. [CrossRef]
16. Choi, H.; Stathatos, E.; Dionysiou, D.D. Photocatalytic TiO$_2$ Films and Membranes for the Development of Efficient Wastewater Treatment and Reuse Systems. *Desalination* **2007**, *202*, 199–206. [CrossRef]
17. Baghdadi, A.M.; Saddiq, A.A.; Aissa, A.; Algamal, Y.; Khalil, N.M. Structural Refinement and Antimicrobial Activity of Aluminum Oxide Nanoparticles. *J. Ceram. Soc. Jpn.* **2022**, *130*, 257–263. [CrossRef]
18. Akyildiz, H.I.; Diler, S.; Islam, S. Evaluation of TiO$_2$ and ZnO Atomic Layer Deposition Coated Polyamide 66 Fabrics for Photocatalytic Activity and Antibacterial Applications. *J. Vac. Sci. Technol. A* **2021**, *39*, 022405. [CrossRef]
19. Pham, K.; Pelisset, S.; Kinnunen, N.; Karvinen, P.; Hakala, T.K.; Saarinen, J.J. Controlled Photocatalytic Activity of TiO$_2$ Inverse Opal Structures with Atomic Layer Deposited (ALD) Metal Oxide Thin Films. *Mater. Chem. Phys.* **2022**, *277*, 125533. [CrossRef]
20. Islam, S.; Akyildiz, H.I. Atomic Layer Deposition of TiO$_2$ Thin Films on Glass Fibers for Enhanced Photocatalytic Activity. *J. Mater. Sci. Mater. Electron.* **2022**, *33*, 18002–18013. [CrossRef]
21. Li, L.; Yu, P.; Li, Y.; Wu, X.; Li, W.; Cheng, X. A Facile Approach to Fabricating Antibacterial Textile with High Efficiency and Compact Process. *Adv. Mater. Interfaces* **2021**, *8*, 2101197. [CrossRef]
22. Popescu, M.C.; Ungureanu, C.; Buse, E.; Nastase, F.; Tucureanu, V.; Suchea, M.; Draga, S.; Popescu, M.A. Antibacterial Efficiency of Cellulose-Based Fibers Covered with ZnO and Al$_2$O$_3$ by Atomic Layer Deposition. *Appl. Surf. Sci.* **2019**, *481*, 1287–1298. [CrossRef]

23. Wang, Z.; Zhang, L.; Liu, Z.; Sang, L.; Yang, L.; Chen, Q. The Antibacterial Polyamide 6-ZnO Hierarchical Nanofibers Fabricated by Atomic Layer Deposition and Hydrothermal Growth. *Nanoscale Res. Lett.* **2017**, *12*, 421. [CrossRef] [PubMed]
24. Nam, T.; Kim, J.M.; Kim, M.K.; Kim, H.; Kim, W.H. Low-Temperature Atomic Layer Deposition of TiO_2, Al_2O_3, and ZnO Thin Films. *J. Korean Phys. Soc.* **2011**, *59*, 452–457. [CrossRef]
25. Aghaee, M.; Maydannik, P.S.; Johansson, P.; Kuusipalo, J.; Creatore, M.; Homola, T.; Cameron, D.C. Low Temperature Temporal and Spatial Atomic Layer Deposition of TiO_2 Films. *J. Vac. Sci. Technol. A* **2015**, *33*, 041512. [CrossRef]
26. Wu, P.; Imlay, J.A.; Shang, J.K. Mechanism of *Escherichia coli* Inactivation on Palladium-Modified Nitrogen-Doped Titanium Dioxide. *Biomaterials* **2010**, *31*, 7526–7533. [CrossRef]